

# A Novel Strategy for Designing and Manufacturing a Fixed Wing MAV for the Purpose of Increasing Maneuverability and Stability in Longitudinal Axis

M. Radmanesh<sup>1†</sup>, O. Nematollahi<sup>1</sup>, M. Nili-Ahmadabadi<sup>1</sup> and M. Hassanalian<sup>1</sup>

<sup>1</sup> Department of Mechanical Engineering, Isfahan University of Technology, Isfahan 84156-83111, Iran

†Corresponding Author Email: [Rezaradmanesh90@hotmail.com](mailto:Rezaradmanesh90@hotmail.com)

## ABSTRACT

In this study, a novel simple strategy is proposed to choose and accommodate an airfoil based on the effects of airfoil type and plan-form shape on the flight performance of a micro air vehicle. In this strategy, after defining flight mission, the weight of the micro air vehicle is estimated and then, aerodynamic parameters and thrust force are calculated. In the next step, some different plan-forms and airfoils are investigated to be selected for decreasing the stall region in high attack angles by open source software named XFRLR5. Having calculated the aerodynamic center, the pitching moment needed to stabilize the micro air vehicle is computed. Due to the static margin, the airfoil camber line is changed to stabilize the micro air vehicle and then, its thickness is improved to reach to a high aerodynamic characteristic. To evaluate the software results, some flight tests are performed which then compared to the software results that show a good agreement. Finally, some adjustments and improvements are made on the micro air vehicle and then, its performance is obtained by the flight tests. The flight test results show it has an excellent aerodynamic performance, stability and maneuverability.

**Keywords:** Airfoil, Design Strategy, MAV, Plan-form, Stability, Maneuverability.

## NOMENCLATURE

$C$	reference chord	$S_h$	horizontal tail area
$C_{lw}$	lift coefficient generated by the vehicle wing	$S_w$	wing area
$C_{lh}$	tail lift coefficient	$T_{SL}$	thrust at sea level while taking off
$C_{mcgb}$	pitching moment around foil center of mass	$W_{TO}$	total weight of air vehicle at takeoff
$C_{macw}$	wing pitching coefficient around the aerodynamic center of gravity	$W_{STR}$	air vehicle structure weight
$C_D$	lift drag coefficient equals zero	$W_{PL}$	weight of air vehicle pay load
$h$	flight height	$W_B$	battery weight
$K_1$	polar second-order coefficient	$W_{PP}$	propulsion weight of air vehicle
$K_2$	polar first-order coefficient	$X_{cg}$	the distance between aerodynamic center and the center of gravity
$L_h$	distance between center of gravity and aerodynamic center of tail	$\alpha$	thrust constant in different flight phases
$n$	lift to vehicle weight in various flight phases	$\beta$	weight ratio in different flight phases
$q$	dynamic pressure	$A_{C/4}$	sweep angle of air vehicle in 0.25 length of chord

## 1. INTRODUCTION

Micro air vehicles (MAVs) are very significant due to their application in civil, military and industry along with their low weight as specific

characteristic. They are unmanned and their sizes are less than 1 meter. According to a defined mission, MAV size with its mounted equipments can vary. Their small sizes compared with the other unmanned air vehicles (UAV) causes the MAVs to

have an extensive operation field. Although their small sizes reduce the structure costs, the related electronic equipments are very expensive. Also, they are of high sensitivity in design and performance because of their small sizes. On the other hand, airfoil design and optimization is very important in aerodynamics because of its significant role in flight. Therefore, the body of a MAV are completely composed of airfoil to have a better performance [Barnhart \*et al.\* \(2004\)](#).

However, MAVs can be categorized into fixed wings, quad rotors, flapping and vertical flier kinds as shown in [Fig. 1](#). They flight like other unmanned air vehicles by remote control because the human attendance is difficult, dangerous or even impossible. With regard to the mentioned specifications, MAVs have a series of potentials for performing some missions like detecting and patrolling. The first research on MAVs was performed in RAND institution. At that work, some multiple studies were done on MAVs smaller than 5 cm which are able to perform detecting and rescuing missions [Torres and Mueller \(2004\)](#).

Because MAVs are very small-size and low speed their Reynolds number are very low that results unique aerodynamic conditions ([Zhang, 2007](#)). On the other hand, the limited wing surface causes the generated lift force to be low. Plan-forms, the top view of MAVs, are in the form of Delta, Zimmerman, Inverse Zimmerman, Rectangular, Elliptical and irregular ones [Anderson, \(2009\)](#). Some different plan-forms are shown in [Fig. 2](#). Aerodynamic optimization of plan-forms increases the aspect ratio of air vehicle incorrectly and impractically ([Obayashi, 1998](#)). In classic planes, the shape of plan-form should be selected in the preliminary steps ([Obayashi, 2000](#)). Because design methods are aimed at improving specific conditions of air vehicle plane, and the proposed design plan can be adapted to other design cycles, some parts are briefly mentioned beforehand.

The first flight was performed by Wright brothers in 1903 ([Liebeck, 2004](#); [Corning, 1953](#)) explained the conceptual design of ultrasound and infrasound passenger air vehicles. The order he used in his air vehicle design was considered as one of the first design documents. Having introduced the amphibious air vehicles, Wood clarified their basics which were the preliminary discussion in this field ([Wood, 1968](#); [Stinton, 1998](#)) described the basics of airscrews and their condition. ([Nicolai, 1975](#)) introduced mass estimation in conceptual design of air combats and ultrasound air vehicles. He is one of the introducers of the economic effects on the air vehicle design. ([Roskam, 1985](#)) suggested a new design procedure in which various variables including aerodynamic, foil, flight dynamic and run force were considered separately. ([Whitford, 1987](#)) analyzed different design procedures of air combats. He evaluated effective variables in air combat performance from the First World War. ([Torenbeek, 1982](#)) investigated the experimental relations of design and suggested a

method to calculate the air vehicle mass. ([Raymer, 2012](#)) proposed a method to increase the air vehicle maneuverability and decrease the drag force in ultrasound flight using the computational fluid dynamic and finite elements. ([Anderson, 2009](#)) evaluated the relations between the air vehicles design and their performance.

The time and energy used in design and examination of air vehicle are very important. Airfoil selection is an important stage of design and has a rigorous effect on the vehicle performance. In MAV design procedure, the aim is to neglect the horizontal tail because, the lower the construction weight, the higher the MAV performance. The massive structures need to have more effective wing span. The aim of MAV construction is to reduce size and weight of air vehicle.

In this research, a procedure is presented to select the MAV airfoil shape without horizontal tail and to study all parameters of airfoil selection. Also, Using the proposed procedure, a vast range of airfoils are evaluated in such a way that the time required for the design and flight tests reduces. In this method like the most design procedures, the trial and flight tests are key components. Having computed the air vehicle weight, it is necessary that the most fitted plan-form be selected for the defined mission. In this paper, a fixed wing MAV would be designed using the proposed method.

Different methods have been developed in order to ease the path for designers to select the needed airplane. The novelty of the proposed strategy lies within the difference of airfoil selection and optimization for mission requirements. The mission requirements could be summarized in the amounts of maneuverability, stability and endurance of MAV in different flight conditions. Each of these has an impact on the flight and also could change the type and size of airfoil. Reformation of airfoil is one of the advantages of this method to maximize the performance of the tailless MAV. Changing the airfoil shape and evaluating the aerodynamic characteristics of the changed shape by using open source software named XFLR5 give designers insight into airfoil selection and design. None of the mentioned strategies discuss the evaluation, optimization and improvisation of airfoil for air vehicles requirements.



**Fig. 1. samples of MAVs**

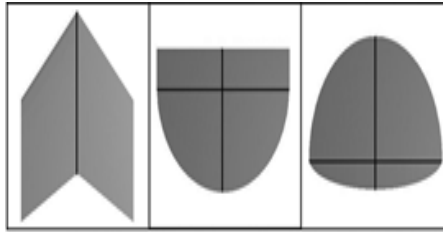


Fig. 2. Samples of Plan-forms

## 2. XFLR5

XFLR5 is open source software which analyzes the aerodynamic characteristics of 3D geometries. As a matter of fact, it is the advanced version of XFOIL software. This software has multiple abilities such as airfoil analysis; planning and drawing wing, foil, tail and the other components. Therefore, it can be used for the aerodynamic analysis and stability control (Deperrois, 2010). In XFLR5, air vehicle is evaluated using one of the three following methods:

- a. LLT (lifting line theory)
- b. VLM (vortex lattice method)
- c. 3D panel

Each mentioned method has its own limitation and preferences. Each wing is defined by multiple panels described with the following parameters:

- a. Length of panel
- b. Chord length of airfoil
- c. Deviation angle of leading-edge at origin and end of panel with respect to the reference line
- d. Dihedral angle
- e. Panel meshing to analyze CLM

## 3. DESIGN METHODOLOGY

As mentioned before, in order to start designing, it is necessary that mission be defined. The mission that the MAV is run into is very important. In other words, the mission represents the loads MAV needs and specifies the mission endurance. Therefore, some weights of the equipments would be varying according to the mission.

Having defined the mission, the MAV weight can be estimated according to the loads induced on it (Gallman, 1993). The results of numerous researches show that the weight must be analyzed to find the form and size of plan-forms (Wakayama, 1995). One way to weight estimation is statistical methods in which the weight is estimated according to the equation between the body and takeoff weight. Using the statistical data and plotting different profiles, it seems there is a linear equation between  $\text{Log}(W_{str})$  and  $\text{Log}(W_{TO})$  of air vehicle. Having weight data of similar air vehicles, drawing the log profiles and calculating takeoff weight in terms of structure weight, a linear equation is concluded as follows.

$$W_{TO} = W_{str} + W_{PP} + W_{PL} + W_B \quad (1)$$

$$W_{str} = xW_{TO} \quad (2)$$

Regarding to the statistical population, Fig.4 has been drawn.

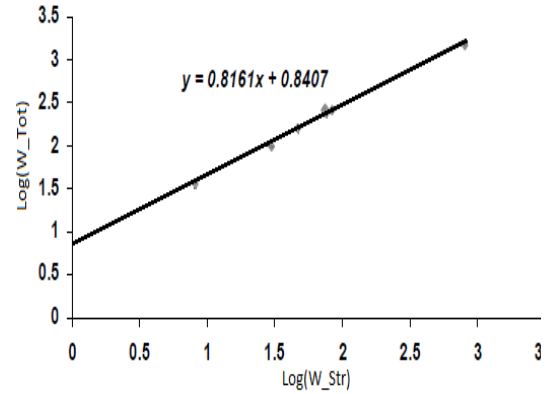


Fig. 4. Statistical diagram for (Log(W\_Str) vs. Log(W\_Tot))

Therefore, for total weight estimation, the  $x$  values should be calculated. Weight of equipments is estimated 300 grams. Also, according to the above profile and database, the structure weight to total weight ratio is estimated 0.33. Considering the fact that the total weight of structure and equipments is the only unknown parameter, its value is estimated 450gr as below:

$$\begin{aligned} W_B &= 120 \text{ g,} \\ W_{PL} &= 140 \text{ g,} \\ W_{PP} &= 110 \text{ g,} \end{aligned}$$

The structure weight is 130gr of which 20gr is considered as the margin error.

## 4. CONSTRAINS ANALYSIS FOR MAV

Forces on a flying MAV including lift, drag, thrust and weight. In this MAV, the drag and thrust forces are in the same lines, with opposite direction. In Fig. 5, the forces on a MAV are shown.

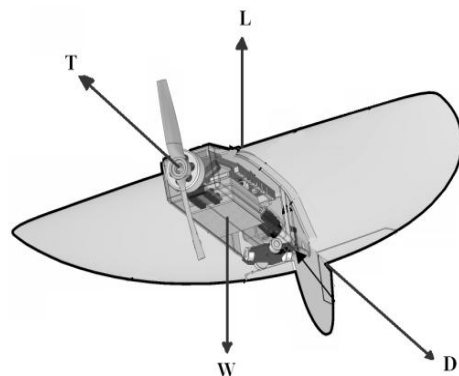


Fig. 5. Forces on MAV

Writing the energy balance equation for MAV, the constraint equation of MAV would be gained.

$$\frac{T_{SL}}{W_{TO}} = \frac{\beta}{\alpha} \left\{ \frac{qS}{\beta W_{TO}} \left[ K_1 \left( \frac{n\beta W_{TO}}{qS} \right)^2 + K_2 \left( \frac{n\beta W_{TO}}{qS} \right) + C_{D_0} \right] + \frac{1}{V} \frac{d}{dt} \left[ h + \frac{V^2}{2g} \right] \right\} \quad (3)$$

The above equation relates the aircraft's wing loading to the thrust one. Eq. (3) would be used for different flight modes. For MAVs with electric motor, simulation is in the form of thrust due to total weight ( $T_{SL}/W_{TO}$ ) on the total wing loading ( $W_{TO}/S$ ). In the following equation  $R_C$ =Radius around,  $dh/dt$  = Ascent velocity,  $dv/dt$ = Acceleration and  $C_{Lmax}$ = Maximum lift coefficient.

**State 1:** Constant altitude/speed cruise,  $P_s=0$

$$\frac{T_{SL}}{W} = \frac{1}{\alpha} \left[ \left( \frac{1}{\pi eAR} \right) \frac{2}{\rho V^2} \left( \frac{W}{S} \right) + \frac{C_{D0}}{\rho V^2} \left( \frac{W}{S} \right) \right] \quad (4)$$

**State 2:** Constant speed climb,  $P_s = dh/dt$

$$\frac{T_{SL}}{W} = \frac{1}{\alpha} \left[ \left( \frac{1}{\pi eAR} \right) \frac{1}{q} \left( \frac{W}{S} \right) + \frac{C_{D0}}{q} \left( \frac{W}{S} \right) + \frac{1}{V} \frac{dh}{dt} \right] \quad (5)$$

**State 3:** Constant altitude/speed turn,  $P_s = 0$

$$\frac{T_{SL}}{W} = \frac{1}{\alpha} \left[ \frac{1}{\pi eAR} \left( 1 + \left( \frac{V^2}{gR_C} \right) \right) \frac{2}{\rho V^2} \left( \frac{W}{S} \right) + \frac{C_{D0}}{\rho V^2} \left( \frac{W}{S} \right) \right] \quad (6)$$

**State 4:** Horizontal acceleration,  $P_s = V/g dV/dt$

$$\frac{T_{SL}}{W} = \frac{\beta}{\alpha} \left[ \frac{1}{\pi eAR} \frac{1}{q} \left( \frac{W}{S} \right) + \frac{C_{D0}}{q} \left( \frac{W}{S} \right) + \frac{1}{g} \frac{dV}{dt} \right] \quad (7)$$

**State 5:** Accelerated climb,  $P_s = dh/dt + V dV/gdt$

$$\frac{T_{SL}}{W} = \frac{1}{\alpha} \left[ \frac{qs}{W} \left[ \frac{1}{\pi eAR} \left( \frac{1W}{qS} \right)^2 + C_{D0} \right] + \frac{1}{V} \frac{d}{dt} \left( h + \frac{V^2}{2g} \right) \right] \quad (8)$$

**State 6:** Hand launching

$$\frac{T_{SL}}{W} = \frac{1}{\alpha} \left[ \frac{1}{\pi eAR} C_{Lmax} + \frac{C_{D0}}{C_{Lmax}} \right] \quad (9)$$

With performance constraint analysis and plotting relevant graphs, ultimately, solution space for MAV design point is determined. In Fig. 6, the presented graph is a constraint analysis of MAV performed by (Hassanalian, 2012).

Having performed analysis and estimated trust force, the wing area can be calculated according the following equation.

$$\frac{T_{SL}}{W_{TO}} = 0.65 \quad (m^2) \quad (10)$$

$$\text{Pay Load} = \frac{W_{TO}}{S} = 35 \quad (N / m^2) \quad (11)$$

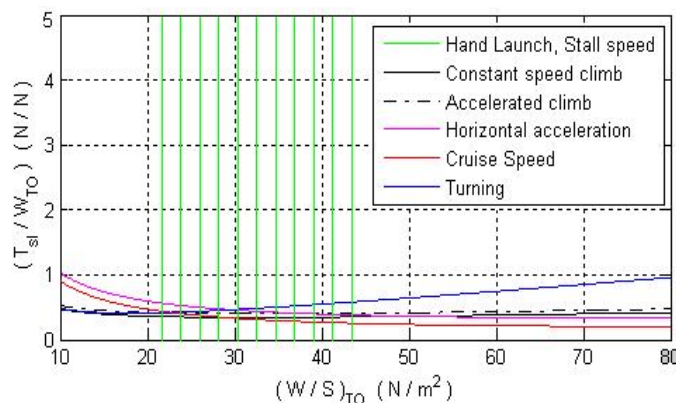


**Fig .6** Constraint analyses for a MAV

Here, some standard plan-forms such as Rectangular, Zimmerman, Inverse Zimmerman, Elliptical, Delta and Morphing are investigated to be considered as our selection. Afterwards, the results of these plan-forms are analyzed using XFLR5 software. The software is validated by comparison between the software results and wind tunnel experimental data. The main aim of this phase is to investigate different plan-forms shapes; therefore, it is necessary that the other parameters be constant. So, the plan-form area and length and, the airfoil type should not be changed. The following parameters are computed from the software to be compared to each other.

- a) Higher lift coefficient
- b) Higher aerodynamic ratio
- c) Higher  $C_{L_{max}}$  and  $\alpha_{C_{L_{max}}}$
- d) More distance from the leading edge to separation boundary
- e) ability to build selective plan-form

Some results of S5020 airfoil obtained from the software are mentioned in Table 1 in which  $C_L$  obtained from zero attack angle. It is evident the differences between  $C_L$  in different plan-forms are more rigorous at higher attack angles. For the above analyses, the sweep back angle for Delta and Inverse Zimmerman plan-forms is assumed 25 degrees to create the best condition for MAV (Mattingly, 2002). Also, for MAV with Plan-form 1, the sweep back angle is 11-12 degrees. The cruise speed is selected 20 m/s based on which Reynolds number is obtained 520000. Considering  $m = 450\text{gr}$ , air density  $= 1.225\text{ kg/m}^3$  and airfoil aspect ratio  $= 1.5$ , the wing area is obtained  $12.6\text{ dcm}^2$ . The plan-form shape with its sizes is shown in Fig. 7.

**Table 1 Plan form performances in the same conditions**

Plan form	$C_L$	L/D	$C_{L_{max}}$	$\alpha_{C_{L_{max}}}$
Zimmerman	0.035	3.45	1.19	55-65
Inv. Zimmerman	0.038	3.64	1.19	55-65
Rectangular	0.034	3.31	1.21	55-65
Elliptical	0.035	3.36	1.18	55-65
Delta	0.034	3.35	1.19	55-65
MAV Plan-form 1	0.039	3.72	1.21	55-65

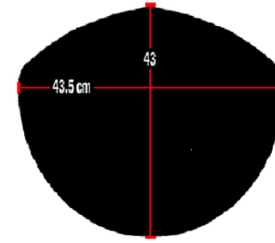


**Fig. 7. Plan-form that used for designing the MAV**

The MAV Plan-form 1 is a modified version of inverse Zimmerman plan-form which was designed by Isfahan University of Technology design team. Now, it is time to choose the appropriate airfoil. Having specified all aerodynamic parameters, the airfoil type can be chosen to meet the prescribed aerodynamic specifications. In cruise speed, the equation is:

$$mg = L = \frac{1}{2} \rho v^2 S C_L \quad (12)$$

Minimum value of 3D lift coefficient calculated from the above equation is 0.143. Therefore, the selective airfoil must satisfy the lift coefficient. All analysis is performed at an angle of attack of 4 degrees. The investigated airfoils are shown in Table 2.

**Table 2 Airfoil tested for the vehicle**

Airfoils	Lift Coefficient	Pitching moment
mh81	0.689	-0.009
s5020	0.592	-0.003
s5010	0.58	-0.004
goe744	0.814	-0.017
fx05h126	0.746	-0.039
ah80136	0.628	-0.01
mh104	0.612	-0.011
B29tip	0.683	-0.035
E169	0.443	0.003

Because of large and non-negligible errors caused by designing equations, introduced by Radmanesh *et al.* (2012), in order to select the airfoils meeting desirable lift coefficient, the flowchart shown in Fig. 8 is used. Another phenomenon of low Reynolds number is flow separation bubble. Flow separation bubble is seen when flow separates from the wing surface near the leading edge and a free shear layer is formed in



laminar flow. If the Reynolds number exceeds a critical value, the air vehicle will encounter an unsteady condition. Little turbulences of the flow lead to turbulent flow in the free shear layer. This free turbulent shear layer causes the flow to be attached the wing surface again. The width of the flow separation bubble is varied between 15% and 40% of airfoil chord line (Mueller 2003). Regarding the mentioned issues, the airfoils work efficiently, if flow separation bubble does not occur

Next step is to find the aerodynamic center on the plan-form. Aerodynamic center is a point located on the plan-form surface around which the lift force moments are zero. The aerodynamic center is estimated for each plan-form related to lift coefficient in low attack angle by using linear regression for gradient of the pitching moment profile (Recktenwald, 2010). Generally, pitching moment is calculated around 25% of chord line from the leading-edge. It is often a negative value (Crook, 2002)

$$C_m = \frac{2M}{\rho C S V^2} \quad (13)$$

If the longitudinal stability of air vehicle is supposed to be investigated, it is necessary to calculate the pitching moment around the center of gravity of air vehicle according to Eq. (14).

$$C_{m_{cg}} = \frac{x_{cg}}{C} C_{l_w} - \frac{l_h S_h}{C S_w} C_{l_h} + C_{m_{acw}} + C_{m_{cgbody}} \quad (14)$$

The pitching moment variation related to the attack angle is called the pitching stiffness ( $C_{m\alpha}$ ). The pitching moment variation versus the wing lift coefficient is defined by Eq. (15).

$$\frac{\partial C_{m_{cg}}}{\partial \alpha} = \frac{x_{cg}}{C} C_{l_{\alpha w}} - \frac{l_h S_h}{C S_w} C_{l_{\alpha h}} + \frac{\partial C_{m_{cgbody}}}{\partial \alpha} \quad (15)$$

The role of horizontal tail for stabilizing their vehicle is symbolically shown in Fig. 9.

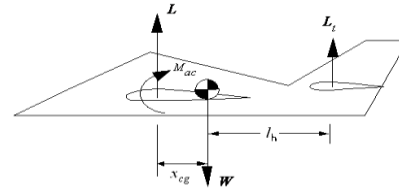


Fig. 9. Longitudinal stability of airplane

For MAVs, the equations are simplified as follows:

$$M = M_0 - x(Lift) \quad (16)$$

$$c_m = c_{m_0} - \frac{x}{l} c_l \quad (17)$$

The Static Margin is defined as below equation:

$$\frac{\partial C_{m_{cg}}}{\partial C_l} = -\frac{x}{MAC} \times 100 = -\text{Static Margin} \quad (18)$$

Therefore, for fixed-wing MAVs without horizontal tail, two scales related to pitching moment are obtained. These parameters are given in Eq. (12) and (13).

$$c_{m_0} > 0 \quad (19)$$

$$\frac{\partial C_{m_{cg}}}{\partial c_l} < 0 \quad (20)$$

With regard to the behavior of  $C_l$  profiles against  $\alpha$ , it is founded that these two parameters are directly related before the airfoil reaches stall. So, it is concluded that:

$$\frac{\partial C_{m_{cg}}}{\partial \alpha} < 0 \quad (21)$$

Therefore, if the static margin is obtained, the distance between AC and CG can be calculated. To achieve  $C_m$  for 3D air vehicle, the cruise state is considered. In this situation, the below equations are obtained writing static equations for air vehicle.

$$W \cdot x = M_{3D} \quad (22)$$

$$\frac{2W}{\rho C S V^2} \cdot x = C_{m_{cg}} \quad (23)$$

Having considered the plan-form, the Static margin is selected 10%. Therefore, according to Eq. (16), the distance between the gravity center and aerodynamic center is 3.8cm. It means that the center of gravity is located 4.166 cm away from the plan form tip. Thus, according to Eq. (21), 3D moment coefficient is 0.0143. To calculate  $C_{m_w}$ , the following equation is used, briefly:

$$C_{m_{cg}} = C_l(x) + C_{m_w} \quad (24)$$

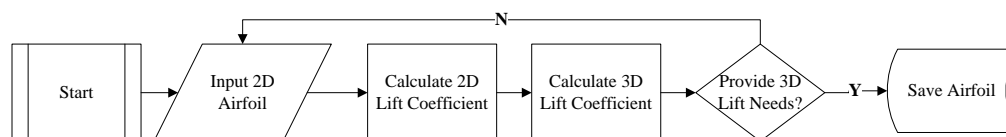


Fig. 8. Chart used to evaluate the airfoil by lift coefficient

Generally, the pitching moment of wing is related to the pitching moment of airfoil. The following Equation (25) relates these two parameters to aspect ratio and sweep angle.

$$C_{mw} = C_{mairfoil} \left( \frac{AR \cos \Lambda_{C/4}}{AR + 2 \cos \Lambda_{C/4}} \right) \quad (25)$$

In which  $\Lambda_{C/4}$  represents the sweep angle of air vehicle at one-fourth of its chord length. With regard to Eq. (17), the pitching moment of airfoil is calculated and then, the following results are obtained.

$$C_{mw} = 8.886 \times 10^{-3} \quad (26)$$

$$C_{mairfoil} = 0.02438 \quad (27)$$

Next step is aimed at calculating the pitching moment of airfoil required to plan air vehicle via reforming airfoil reflex. Also, with regard to the limitations of plan such as airfoil thickness, little reformation can be applied to the final airfoil

geometry. To reduce instability around the pitching axis of airfoil, it is necessary to change the airfoil geometry. Final purpose of this stage is to achieve an airfoil with optimal performance by changing the airfoil reflex which causes its pitching moment to be changed. Also, changing the flap angle and its location changes the pitching moment. Moreover, changing the airfoil pitch leads the aerodynamic coefficients to be changed. It is worthy to noting that pitching moment coefficient increases when flap angle changes to negative values. So effect of thickness on the selected airfoil is valuated and showed in Fig. 10. With regard to drawn profile, and the mission requirements, the raw airfoil thickness is considered as 9%. After that the raw airfoil thickness was selected, next step for adapting airfoil on micro air vehicle is to increase the pitching moment by changing airfoil geometry via flapping. The diagram of this action is shown in Fig. 11 and Fig. 12.

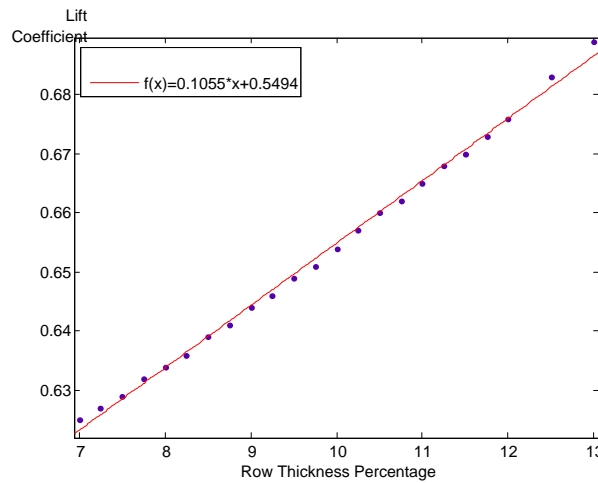


Fig. 10. Lift coefficient vs. row thickness percentage

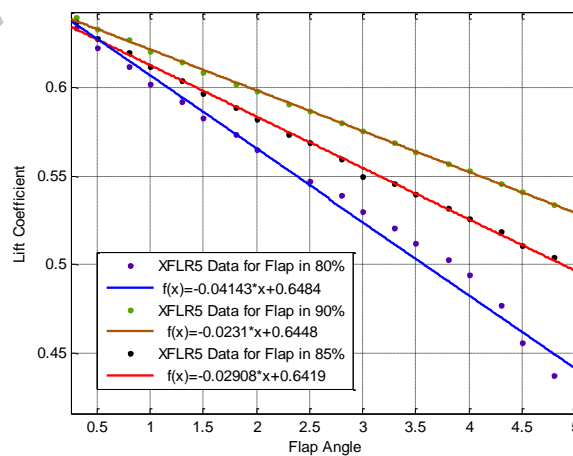
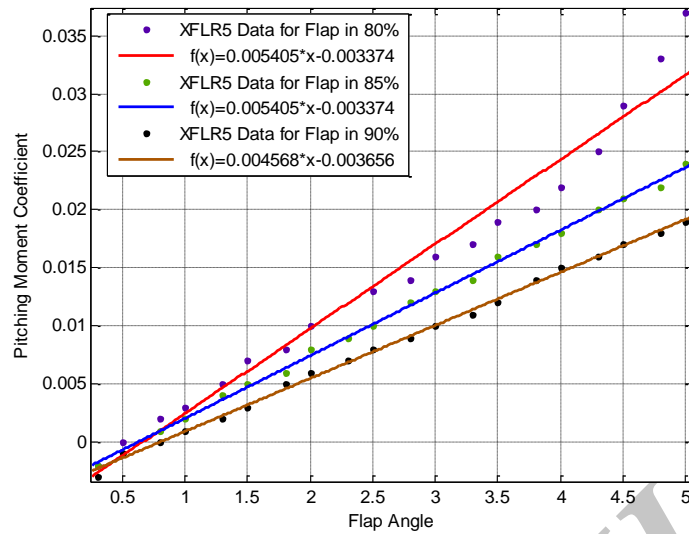


Fig. 11. Effect of flap angle on lift coefficient



**Fig. 12. Effect of flap angle on pitching moment coefficient**

From these profiles, it is obvious that increasing the flap angle of tail leads to the pitching moment increment and lift coefficient reduction. As documented from plots, to meet pitching moment at 85% of Chord line and 50% of airfoil location, a pitching moment coefficient of 0.02438 is obtained at flap angle of 5 degrees.

After considering the volume coefficient of the vertical tail to be 0.6 and defining the tail place, elevators exact location and their area, the final step of our design is performed.

Therefore, we can determine the best airfoil according to the MAV performance obtained from flight test. The related steps are classified in Fig. 13, briefly. It is worthwhile noting that in the most cases flight test is recommended and wind tunnel test is avoided because there are more differences between wind tunnel test used for low Reynolds numbers and flight test used in turbulent and instable flows according to Watkins researches (Watkins, 2010.) The result of this designing and ready for flight test is shown in Fig. 14.



**Fig. 13. Ready to fly tests MAV**

## 5. EXPERIMENTAL FLYING TESTS

As the final stage of MAV designing some flying test should be carry out. The main goal of the proposed procedure is maneuverability of MAV through the flight. For tracking this goal and showing efficiency of the procedure, a control system was installed on MAV and data of flight was collected.

The main purpose of using a control system during the flight is to stabilize the aircraft after being disturbed from its wing-level equilibrium flight attitude. In this study, by using a Gyro sensor and the control circuit, the longitudinal angle of MAV has been measured. Block diagram of the angle measurement system is shown in Fig. 15.

The main reason of measuring the longitudinal angle is to find out the efficiency of the proposed cycle. The Gyro sensor has been normally placed on the wing with the angle of 4 degrees and this angle has been considered as the level angle. Sensors data has been saved every 0.5 second and plotted for each flight test. Flight tests include hand launch, increasing altitude, cruise flying and landing. Flight tests has been done in the condition mentioned below:

- a) Wind Velocity= 2m/s
- b) Humidity= 5%
- c) Height from the sea=1400m

### 5.1 Flight Test Analyses

It is important to mention that in the MAV designed with the proposed procedure, aircraft motor was alimented in 4 degrees with horizontal line. So while aircraft is in normal performance and fly on horizontal line, Gyro sensor shows 4 degrees.



Therefore, the best longitudinal stability should be occurs on the mentioned degree.

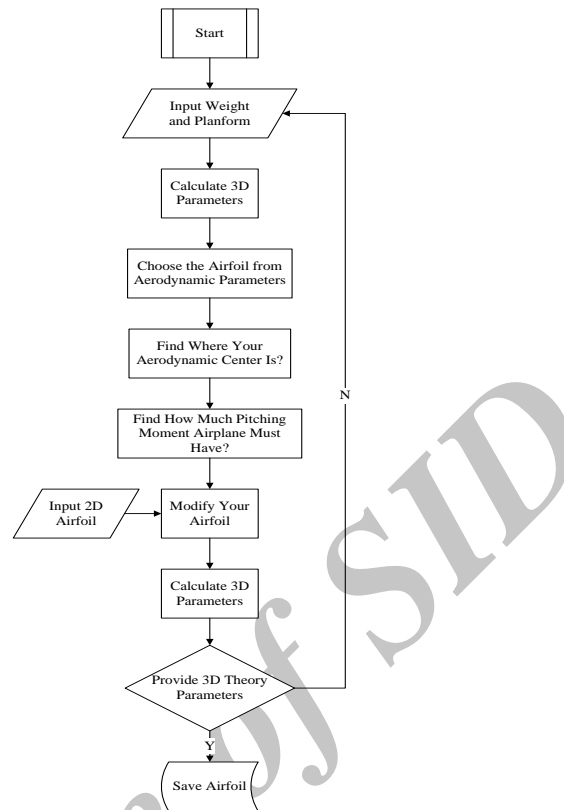


Fig. 14. Designing chart

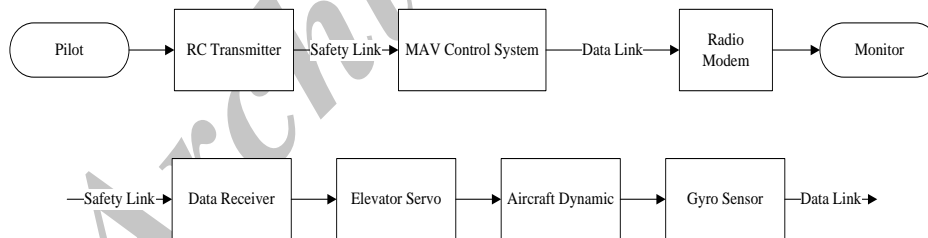


Fig. 15. Block diagram of the angle measurement system

Flight Test No. 1: In this Test the designed MAV has done a nose up flight, which means the MAV has not been stabilized longitudinally. The Longitudinal behavior of MAV has shown in Fig. 16.

Flight Test No.2: In this test The MAV has shown the behavior as flight test No.1 and it has been plotted in Fig.17.

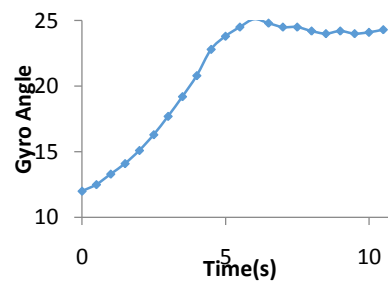
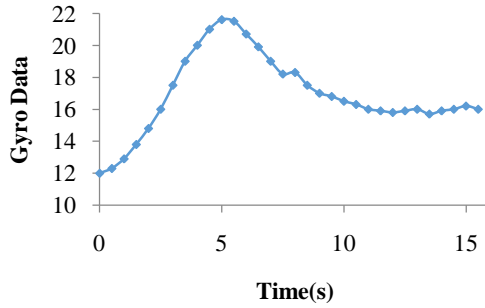
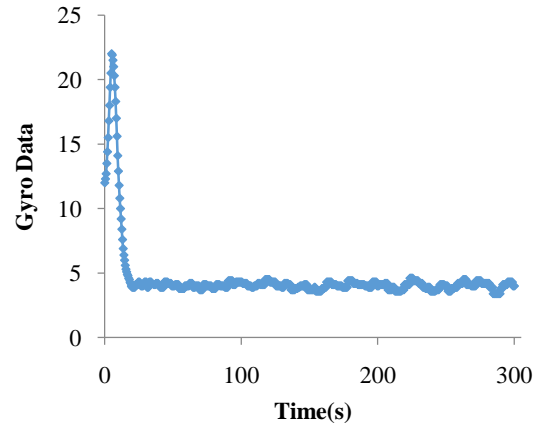


Fig. 16. Flight Test No. 1



**Fig. 17. Flight Test No. 2**



**Fig. 18. Flight Test No. 3**

The main reason that the MAV behaves Nosed up in the longitudinal axis is that the static margin entered as an input to the cycle, was inappropriate. Flight Test No.3: In these Flight tests the MAV shows an ideal behavior longitudinally. The Gyro sensor data has been plotted in Fig.18. Data has been gained just for the cruise mode.

In this test, the MAV performed the level flight, perfectly. The flight tests results are shown in Table 3. The final manufactured MAV is shown in Fig. 19

**Table 3 Flight test results**

No	Duration of test	Problem	Correction	Aerodynamics	Stability	Maneuverability
1	12 seconds	Nose Up Fly	Moving the center of gravity forward about 2cm	-	-	-
2	16 seconds	Nose Up Fly	Moving the center of gravity forward about 1cm	-	-	-
3	5 minutes	Fly Normally-trim of elevators	-	Ok	Ok	-
4	6 minutes	Fly Normally-trim of elevators	-	Ok	Ok	Ok



**Fig. 19. Output of the designing cycle**

## 6. CONCLUSION

The methodology proposed in this research, showed that the time for designing and manufacturing the fixed wing MAV decreases enormously. Also, a novel method was presented to stabilize the fixed wing MAV longitudinally by changing airfoil geometry. Finally, MH81 was selected as the optimum airfoil. Some changes were applied in row thickness to reach the designing purpose and aerodynamic requirements. Also, the reflex of the airfoil was changed to improve the pitching moment. The research results were obtained in  $Re=520000$ . The results proved the efficiency of the proposed methodology.

## ACKNOWLEDGEMENTS

This Investigation is sponsored by Isfahan University of Technology and Khodran Vafa Co. to attend in IMAV2010 competition held in Germany. The MAV gained the Forth place during the competition.

## REFERENCES

- Anderson, D.W., Eberhardt, S., 2009. *Understanding Flight*, Second Edition. McGraw-Hill Companies, Incorporated.
- Barnhart, F., Cuipa, M., Stefanik, D., Swick, Z., 2004. Micro-Aerial Vehicle Design with Low Reynolds Number Airfoils. Brigham Young University.
- Cherne, J., Culick, F.E.C., Zell, P., 2000. The AIAA 1903 Wright'Flyer'Project Prior to Full-Scale Tests at NASA Ames Research Center, Proc. of AIAA 38th Aerospace Sciences Meeting.
- Corning, G., 1953. *Supersonic and subsonic airplane design*. Edwards Bros., Ann Arbor, Mich.
- Crook, A., Gerritsen, M., Mansour, N., 2002. An experimental investigation of high aspect-ratio rectangular sails, *Annual Research Briefs*. Center for Turbulence Research, Stanford University.
- Deperrois, A., 2010. XFLR5 Analysis of foils and wings operating at low reynolds numbers, 2009. Available from: <http://xflr5.sourceforge.net/xflr5.htm> [Accessed 19 February 2010].
- Gallman, J.W., Smith, S.C., Kroo, I.M., 1993. Optimization of joined-wing aircraft. *Journal of Aircraft* 30, 897-905.
- Hassanalain, M., Ashrafizaadeh, M., Ziaei- Rad, S., Radmanesh, M.R., 2012. A new Method for Design of Fixed Wing Micro Air Vehicle, *IMAV 2012, Germany*.
- Liebeck, R.H., 2004. Design of the blended wing body subsonic transport. *Journal of Aircraft* 41, 10-25.
- Mattingly, J.D., Heiser, W.H., Pratt, D.T., 2002. *Aircraft Engine Design*, Second Edition. *Amer Inst of Aeronautics &*
- Mueller, T.J., DeLaurier, J.D., 2003. Aerodynamics of small vehicles. *Annual Review of Fluid Mechanics* 35, 89-111.
- Nicolai, L.M., 1975. *Fundamentals of aircraft design*. Nicolai : distributed by School of Engineering, University of Dayton.
- Obayashi, S., Nakahashi, K., Oyama, A., Yoshino, N., 1998. Design optimization of supersonic wings using evolutionary algorithms, Proc. 4th ECCOMAS *Computational Fluid Dynamics Conf*, 575-579.
- Obayashi, S., Sasaki, D., Takeguchi, Y., Hirose, N., 2000. Multiobjective evolutionary computation for supersonic wing-shape optimization. *Evolutionary Computation, IEEE Transactions on* 4, 182-187.
- Radmanesh, M.R., Hassanalain, M., Fegghi, S.A., NiliAhmadabadi, M., 2012. Numerical Investigation of Azarakhsh MAV, *IMAV2012, Germany*.
- Raymer, D.P., 2012. *Aircraft Design: A Conceptual Approach*. *Amer Inst of Aeronautics &*
- Recktenwald, B.D., Crouse, G.L., Ahmed, A., 2010. Experimental Investigation of a Circular-Planform Concept Aircraft. *Journal of Aircraft* 47, 887-894.
- Roskam, J., 1985. *Airplane Design: Preliminary configuration design and integration of the propulsion system*. Design Analysis & Research.
- Stinton, D., 1998. *The anatomy of the airplane*. American Institute of Aeronautics and Astronautics.

- Torenbeek, E., 1982. Synthesis of Subsonic Airplane Design: An Introduction to the Preliminary Design of Subsonic General Aviation and Transport Aircraft, with Emphasis on Layout, Aerodynamic Design, Propulsion and Performance. *Springer*.
- Torres, G.E., Mueller, T.J., 2004. Low-aspect-ratio wing aerodynamics at low Reynolds numbers. *AIAA journal* 42, 865-873.
- Wakayama, S., Kroo, I., 1995. Subsonic wing planform design using multidisciplinary optimization. *Journal of Aircraft* 32, 746-753.
- Watkins, S., Abdulrahim, M., Marino, M., Ravi, S., . Flight Testing of a Fixed Wing MAV in Turbulence with Open and Closed Loop Control, *IMAV 2010*, Germany.
- Whitford, R., 1987. *Design for air combat. Jane's*.
- Wood, K.D., 1968. *Aerospace Vehicle Design*, Volume I, Aircraft Design, 3 ed. Johnson Publishing, Boulder, Colorado.
- Zhang, X.Q., Tian, L., 2007. Three-Dimensional Simulation of Micro Air Vehicles with Low-Aspect-Ratio Wings. *Key Engineering Materials* 339, 377-381.

Archive of SID